

# Modeling The Hyperloop With COMSOL Multiphysics® : On The Design Of The EPFLoop Pressurized Systems

Zsófia Sajó<sup>1</sup>, Lorenzo Benedetti<sup>2</sup>, Nicolò Riva<sup>3</sup>

EPFL and EPFLoop, <sup>1</sup>M.Sc. Student in Materials science STI,

<sup>2</sup>GEL - GeoEnergy Laboratory ENAC, <sup>3</sup>SCIIC BD - Applied Superconductivity STI

**Abstract:** The EPFLoop team from Ecole Polytechnique Fédérale de Lausanne has developed a capsule thanks to which it won the 3rd place in SpaceX's Hyperloop Pod Competition in 2018. COMSOL Multiphysics was used to analyze and study the pressurized systems of the pod. Three pressure vessels (PVs) of different shape and structure are used to store electrical components in a pressurized environment at 1 bar, meanwhile the external environment is at 8 mbar.

The PVs' failure under load was studied using a stationary simulation and shell finite elements in order to represent the plies of carbon fiber-epoxy and foam. The load conditions were the maximum deceleration (2.6 g), the weight of the internal components and the internal pressure of 1 bar. The aim was to design the plies layering with a minimum Tsai-Wu safety factor of 2 everywhere.

A parametric sweep was then performed to estimate the maximum allowable working pressure (MAWP, corresponding to a safety factor equal to 2) and the BURST pressure (pressure for which the safety factor is less equal than 1 and failure is imminent).

To ensure the normal functioning of electronic components, analyses were done to ensure that the temperature inside the PVs wouldn't be greater than 50°C due to internal electronic heat loads.

This has been done by coupling the Heat Transfer in Solid Module with the Laminar Flow Module in order to take into account convection effects. The simulations were validated by measurements during experimental tests. Experimental results confirmed the design and analyses carried out using COMSOL Multiphysics®.

**Keywords:** Hyperloop, SpaceX, EPFL, EPFLoop, Composites, Carbon Fiber, Pressurized Systems, Safety, Competition

## 1. Introduction

At the 2018 Hyperloop Pod Competition, the EPFLoop team from Ecole Polytechnique Fédérale de Lausanne used composite pressurized systems to store electronic components in a pressurized environment during the run of the Hyperloop pod in vacuum. The team faced challenges both in the design of the pressurized systems structure and in the analysis of their behavior in the presence to heat loads during the run. The aim of the pressure vessels (PVs) is to avoid a direct exposure of sensitive components, such as electronics or batteries, to the vacuum, which would be destructive for such

components. The composite structure of the PVs should safely resist to the conditions in vacuum during the run. On the other side, in order to maintain high performance, low weight should be guaranteed. In order to find such an arrangement, a structural analysis was done.

To ensure the safe functioning of the electronics inside the PVs, the temperature must not exceed 50°C. A thermal analysis has been done to ensure that the PVs will not overheat due to power losses at full power.

## 2. Governing equation

### a. Structural analysis

The structural behavior of the composite carbon fiber and foam pressure vessels is described using shell finite elements, representing the various plies of material. The analysis is carried out under plane stress assumptions and stationary conditions. If the stress in the shell is represented by the tensor  $\sigma$ , then the equilibrium equation is described by:

$$\nabla \cdot \sigma + F_v + 6(M_v \times n) \frac{z}{d} = 0 \quad (1)$$

where  $z$  is the local coordinate through the thickness of the shell,  $d$  is the thickness,  $n$  is the normal to the shell and  $F_v$  and  $M_v$  are respectively the applied force and moment to the shell. In turn, the stresses are defined from the Green-Lagrange strains as function of the degrees of freedom displacement  $u$  and rotation  $a$  [1]. In order to take into account the contribution of various plies,  $u$  and  $a$  are shared between all the plies. Moreover, the orientation of the fibers is defined by the local axis reference, which allows to define precisely the distribution and characteristics of the layers.

The carbon fiber-epoxy plies were modelled assuming an orthotropic material. For this type of material, a quadratic failure criterion may be introduced [2] and, in its general form reads:

$$f(\Sigma) = a_{ij}\sigma_{ij} + b_{ijkl}\sigma_{ij}\sigma_{kl} \leq 1 \quad (2)$$

There,  $f(\Sigma)$  is the expression built on the stress tensor  $\Sigma$ ,  $a$  and  $b$  are experimentally determined material strength parameters.

The Tsai-Wu criterion is part of this category. It is used in the case of plane stress: the stress is located in the plane identified by the axes of orthotropy  $l$  and  $t$ , parallel to the ply. This assumption is valid for thin shells, i.e. its thickness is significantly smaller

that its length and width. The Tsai-Wu failure criterion expression reads:

$$a_{ll}\sigma_l + a_{tt}\sigma_t + B_l\sigma_l^2 + B_t\sigma_t^2 + B_o\sigma_l\sigma_t + B_{lt}\tau_{lt}^2 \leq 1 \quad (3)$$

There  $\sigma_l$  and  $\sigma_t$  are failure strength values, and  $B_o$  is a coupling term used to optimize the orientation of the ellipsoid constituting the failure envelope in axes  $(\sigma_l, \sigma_t, \tau_{lt})$ . The default value of  $B_o$  is -1 [2]. Similarly, each principal stress in the fiber was considered and compared to their respective strength. Hence, the failure criterion reads:

$$(\Sigma) = \frac{\hat{\sigma}_i}{\hat{\sigma}_i} \leq 1 \quad (4)$$

where  $\hat{\sigma}_i$  is the principal stress and  $\hat{\sigma}_i$  is the strength in the i-th direction. The Tsai-Wu safety factor and failure criterion and principal stresses were useful to determine the structural strength for the given configuration of plies. In addition, in order to avoid any interference between the deformation of the pressure vessels and other components of the pod, the total displacements are computed and compared to the maximum clearance available.

### b. Thermal analyses

In the main pressure vessel (MPV), the thermal profile in air and in carbon fiber-epoxy has been simulated according to the estimated thermal load. The heat transfer equations are coupled with the incompressible Navier-Stokes equations from fluid dynamics. The time-dependent heat transfer equation solving the physical condition in the MPV is [4]:

$$\rho C_p \left( \frac{\partial T}{\partial t} + \mathbf{u} \cdot \nabla T \right) + \nabla \cdot (-k \nabla T) = Q \quad (5)$$

Where  $\rho$  is the mass density,  $\mathbf{u}$  the velocity field,  $k$  the thermal conductivity and  $Q$  the heat source given by the electronic heat loads in the MPV. The incompressible Navier-Stokes equations consist of a momentum balance (a vector equation) and a mass conservation and incompressibility condition [4]:

$$\frac{\partial \mathbf{u}}{\partial t} + \rho \mathbf{u} \cdot \nabla \mathbf{u} = -\nabla p + \eta \nabla^2 \mathbf{u} + \mathbf{F} \quad (6)$$

$$\nabla \cdot \mathbf{u} = 0 \quad (7)$$

The analysis of the coupled thermal-fluid model provides the velocity field, pressure distribution, and temperature distribution in the fluid.

The equations are strongly coupled as free convection is added to the fluid flow with the Boussinesq approximation. This approximation assumes that the density does not vary with the temperature. It is considered that the variations of temperature give rise to a buoyancy force lifting the fluid. Therefore, the coupling is also given by the

volumetric force term  $\mathbf{F}$  in the incompressible Navier-Stokes equations. At the same time, the heat equation must account for the velocity field. The velocity field from the laminar flow that determines the convective heat transfer [4] appears automatically as a predefined option in the model input.

### 3. Geometry of the pressure vessels and dimensions

In Fig. 3.1 and Fig. 3.2, the manufactured LPVs and MPV can be seen. The dimensions of the PVs are in Table 3.1.

Table 3.1 – Rough dimensions of the PVs.

Lateral Pressure Vessels	
Length	150 cm
Width	18 cm
Height	28 cm
Main Pressure Vessel	
Length	68 cm
Width	25 cm
Height	30 cm

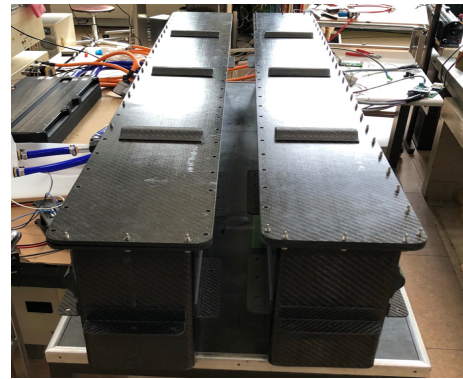


Figure 3.1 - Manufactured lateral pressure vessels.

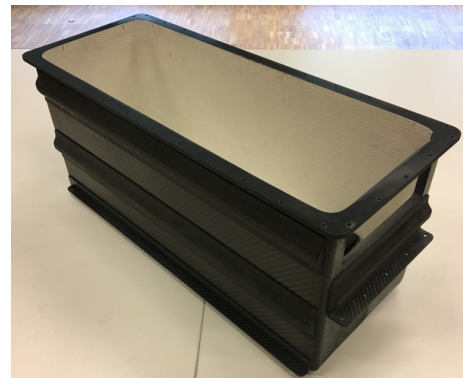


Figure 3.2 - Manufactured main pressure vessels.

### 4. Structural analysis: failure of PVs under loads

The PVs are composed of plies of bidirectional carbon fiber-epoxy composite, a material which combines strength and light weight.

The structural analysis aims to ensure that the stress on any point of the PVs is lower than half of the yield strength of the materials for the chosen configuration of plies in order to obtain a structure which respects the SpaceX safety guidelines [3]. In order to take into account the multiaxial load and response of the material, the Tsai-Wu safety factor and principal stresses are considered, as discussed before.

### a. Geometry, mesh, solver and settings

The plies of carbon fiber-epoxy composite were considered as an orthotropic material and the foam as an isotropic material. The PVs are subjected to an internal pressure of 1 bar. As they are in partial vacuum (8 mbar), the load is assumed to be 1 bar, neglecting the external pressure. The weight of the components inside respectively the central and each lateral PV is 40 kg and 42 kg. The forces corresponding to these weights are applied to the bottom of the PVs. Prescribed displacements were applied to surfaces where the PV is in contact with other components via flanges.

The mesh used was unstructured: although most of it was mapped mesh, free triangular elements were introduced on the corners, where it was not possible to form quadratic ones. The quality of the mesh has been evaluated by skewness which was close at 1 in most of the regions (Fig. 4.1).

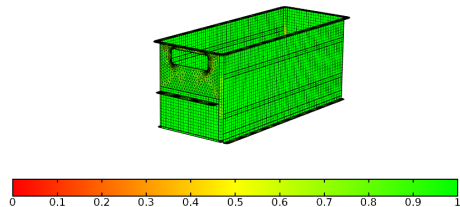


Figure 4.1 - Mapped and free triangular mesh quality measured by skewness.

### b. Results

The first simulation has been carried out applying the internal pressure load of 1 bar, the deceleration and the weight of the internal components. The aim was to find the stationary configuration of plies corresponding to a safety factor of 2 everywhere. In an iterative process, plies were added to the areas where the Tsai-Wu safety factor of 2 was not reached. At each iteration of the stationary simulation, areas with the highest principal stresses were reinforced with more shells until the safety factor reached 2 in the area.

Due to the volume of the inner components and the objective of reducing the weight of the entire pod, the evaluation of the thickness of the reinforcements was necessary: some areas of the PVs required removing the foam layers.

As a consequence, a careful placement of the sandwich structure and, in some areas, a

reinforcement with composite ribs had to be considered. As a result, the sides of the lateral PVs are reinforced with foam. In the case of the MPV, the lack of room has led to the use of supplementary plies of carbon fiber on the walls instead of foam, whereas the bottom of the box is a sandwich structure. A larger deformation may occur in the zones where the surface is less constrained, therefore on the sides of the PVs. The lateral and top/bottom faces are significantly long and there is a risk of inflation of such regions, with unwanted contact with other elements of the pod or even damage of the PV or of other elements. The solution has been to add omega-shaped foam ribs placed on the outside of both PVs. In Fig. 3.1 and Fig. 3.2 is possible to observe these ribs on the lid of the LPV and on the side of all the pressure vessels.

Eventually, the parameters MAWP and BURST had to be estimated [3]. At the MAWP the safety factor has to be superior to 2 everywhere; at the BURST pressure, the entire structure fails as in the case of a thermal runaway which causes abrupt increase of pressure. Therefore, it is assumed that the BURST pressure correspond to the case in which the safety factor is lower than 1 in any region. The pressure inside each PV was varied from 1 to 4 bar with increments of 0.2 bar. A study of the principal stresses was done in order to understand the types and directions of failure.

The parametric sweep showed the weakest regions of the PVs' final structure for the studied plies. The bottom of each PV, where the load is concentrated, is the most vulnerable. In Fig. 4.3 can be seen in both the internal and external plies: the Tsai-Wu safety factor is the lowest in these areas (Fig. 4.3).

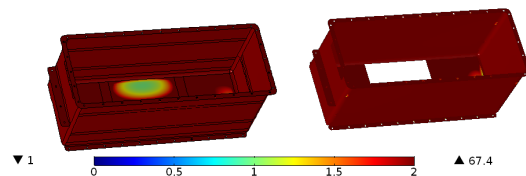


Figure 4.2 - Tsai-Wu safety factor [-] at an internal pressure of 2.6 bar (BURST) on the inner and outer plies (respectively  $x=0$  and  $x=1$ ).

The values in Fig. 4.3, are the minimum Tsai-Wu safety factor calculated during the sweep parameter, for various pressure inside each PV.

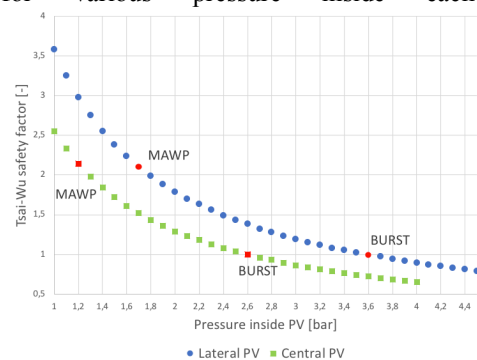


Figure 4.3 - Minimum Tsai-Wu safety factor [-] vs. pressure [bar] inside the central and lateral pressure vessel. BURST and MAWP are represented.

Principal stresses have been studied at MAWP and BURST pressures, for example in Fig. 4.4 are shown the principal stresses of the LPV at BURST. The results are characteristic of a multiaxial problem, where in the case of two plies at opposite and equal distance from the center of the stack, if one is in tension, then the other one is in compression.

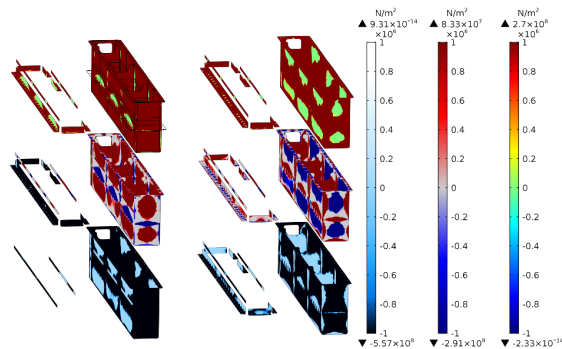


Figure 4.4 – Principal stresses 1, 2, 3 (top to bottom) at 3.6 bar (BURST pressure) on the external and internal ply (left to right).

The structural integrity of the PVs was validated experimentally by injecting air into the sealed PVs through a valve (Fig. 3.5 and 3.6). The value of the pressure on the figures is absolute and, although the pressure is of 2.6 bar at the peak, the one that the pressure vessels were withstanding was 1.6 bar at maximum, which is still in the safety region according to the simulation.

Being that the pod and therefore the PVs will stay in vacuum for long periods, leakage tests have been done to ensure that the leakages were acceptable. Figures 3.5 and 3.6 are the results of the test carried out at EPFL. The leakages are of 22 mbar/h for the LPV and 4 mbar/h for the MPV, therefore the electronics and the batteries will work without being affected by problems due to the exposure to vacuum.

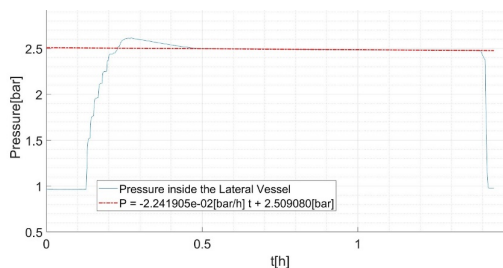


Figure 4.5 - Leak test of a lateral pressure vessel.

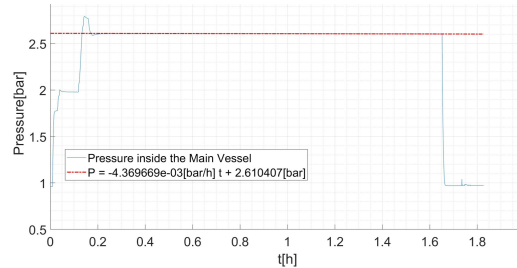


Figure 4.6 - Leak test of the main pressure vessel.

## 5. Thermal analyses

In the model, the heat loads considered are a volumetric heat source and a boundary heat source. The initial temperature is  $T_0 = 40\text{ }^\circ\text{C}$ , given the average temperature at the competition (in Los Angeles, in July). Two analyses have been carried out:

1. Estimation of the maximum temperature reached in vacuum during 40 minutes during which the pod will stay in the tube before the run (also called *idle mode*).
2. Estimation of the maximum temperature reached during the run in about 15 seconds.

The losses for each of the electronic components placed in the main PV are provided in Table 4.1.

Table 5.1 – Heat loads applied on the MPV.

Device	Losses in idle mode [2400 s]	Losses during run [16 s]
Aux Battery	-	1 W
UPS	4.5 W	4.5 W
Sensors	12 W	12 W
CRio	3.4 W	60 W
Pump	-	18 W
VSI	-	6 kW
PCB	1 W	1 W

A simplified geometry has been used in order to avoid complexities due to the CAD of the MPV and consequently benefit the performance of the final mesh (Fig. 5.1). The geometries inside the MPV are electrical components which were considered as a heat source dissipating power (Table 5.1).

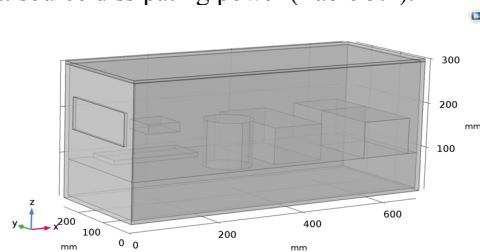


Figure 5.1 - Simplified geometry for the thermal analysis.

### a. Study of the maximum temperature inside the PVs in idle mode

The first analysis had the objective of determining the maximum temperature reached in vacuum during idle mode. A heat transfer model in solids has

been coupled with a laminar flow simulation, to take into account the convection effects. The results show an increase of 5 to 6 °C with respect to the baseline, in both the carbon fiber structure and the temperature of the air in the box.

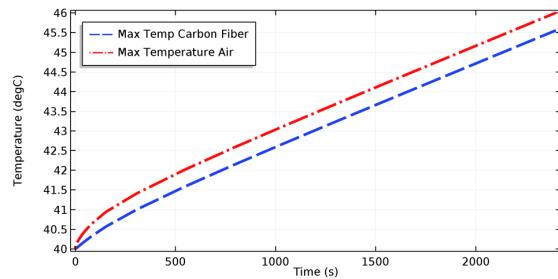


Figure 5.2 - MPV temperature profile during 40 minutes.

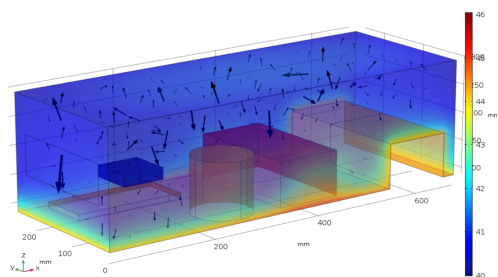


Figure 5.3 - Temperature map [°C] and buoyancy flow due to free convection in the main PV after 2175 s, in the analysis of 40 minutes in the tube.

In Fig. 5.3, the instauration of convective motion inside the MPV around 2000 s can be seen.

### b. Study of the maximum temperature inside the PVs during the run

The aim of the previous simulation was to estimate the thermal profile in the main pressure vessel during the idle mode. The maximum temperature during the run is reached in about 15 seconds. Due to the very short time, free convection can be neglected and only heat transfer in solids is considered. Instead of giving the temperature map inside the MPV, obtained by the previous simulation, the final maximum temperature is given as an input. This temperature is the worst case scenario.

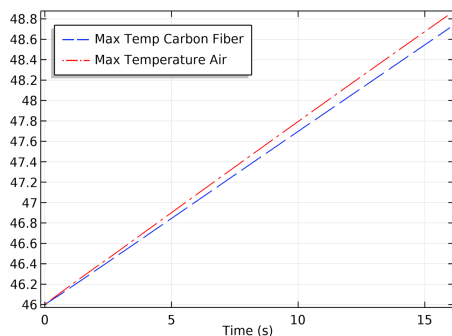


Figure 5.4 - MPV temperature profile during the run.

The temperature at the end of the run is approximately 8°C higher than the initial temperature in the first simulation. It was not certain which was going to be the initial temperature during the competition, so this temperature was considered as the worst-case scenario. According to the simulation, there will be some margin in temperature for the electronics to be working in the proper regime. Moreover, if the temperature would be lower, the margin will be larger because the increase of temperature would still be around 8 °C.

Additionally, the heat capacity of the other metallic components inside the MPV is not considered.

Experimental results are available thanks to the telemetries obtained during the run in tube. Starting from a temperature of 30 °C, the maximum temperature achieved after 60 min in idle mode and 10 s of run is 37 °C.

## 6. Conclusion

The structural analyses have resulted in a safe design of the PVs, which has been confirmed by the thermal analysis. The PVs have been successfully tested at nominal pressure (1 atm). The leakage tests have been successful and encouraging, confirmed also during the real run and tests carried out at the SpaceX facilities. The thermal profile inside the main pressure vessel never rose above 38 °C during the run (resulting in a temperature increase comparable to the one in the simulations above). This work pointed out how interdisciplinary and polyhedral skills can lead to new solutions in engineering. EPFLoop, thanks to COMSOL and others partners, will participate at the 2019 SpaceX Competition.

The authors would like to acknowledge the support of EPFL, FEE, COMSOL and the invaluable collaboration of Cyril Dénéreaz (LMM-STI-EPFL).

## 7. References

- [1] Bathe K.J. (1996). *Finite element procedures*, Prentice-Hall, Englewood Cliffs, NJ
- [2] Gay D. (2015). *Composite Materials Design and Applications*, Boca Raton, FL, CRC Press
- [3] SpaceX, 2018, *Safety Document for SpaceX Hyperloop Competition 2018*
- [4] COMSOL, *Heat Transfer by Free Convection*, 2010 COMSOL AB